Tubular cell-specific platelet-derived growth factor-B drives formation of fibrogenic niches in kidney fibrosis

Check for updates

OPEN

Barbara Mara Klinkhammer[1], Eva Miriam Buhl[1,2], Tim Caspers[1], Sidrah Maryam[3], Dickson W.L. Wong[1], Michael Goedertier[1,4], David Laurin Hölscher[1,3], Roman David Buelow[1], Rafael Kramann[3], Sikander Hayat[3], Jürgen Floege[3] and Peter Boor[1,2]

[1]*Institute of Pathology, RWTH Aachen University Hospital, Aachen, Germany;* [2]*Electron Microscopy Facility, RWTH Aachen University Hospital, Aachen, Germany;* [3]*Division of Nephrology and Immunology, RWTH Aachen University Hospital, Aachen, Germany; and* [4]*Institute for Computational Genomics, RWTH Aachen University Hospital, Aachen, Germany*

Abstract

Introduction: Kidney fibrosis is the underlying pathological process of chronic kidney disease, a major global medical challenge. In most diseases, fibrosis-initiating injury affects epithelial cells. However, the fibrosis-executing cells are interstitial mesenchymal cells, particularly fibroblasts, expressing the platelet-derived growth factor (PDGF) receptor β (PDGFR-β). Here, we analyzed the cell-specific functional relevance of the PDGFR-β ligand, PDGF-B, in the cellular crosstalk in kidney fibrosis.

Methods: Following a transcriptome-wide gene expression analysis of PDGF-B in murine and human kidney tissues, we generated transgenic mouse lines with deletion of *Pdgfb* in major cellular sources of PDGF-B and analyzed kidney phenotypes and fibrogenesis in different kidney fibrosis models.

Results: Mice with *Pdgfb* deletion in kidney tubular epithelial cells showed smaller kidneys and slightly altered microstructure revealed by pathomics, without affecting the overall development or kidney function, even at high age (100 weeks). In three models with tubular injury of different etiologies (ureteral obstruction, ischemia/reperfusion and adenine-enriched diet), mice lacking *Pdgfb* in tubular cells had significantly and specifically reduced activation and proliferation of peritubular PDGFR-β^+ cells and fibrosis. Single-cell expression and cell-cell interaction analysis revealed a paracrine PDGF-B/PDGFR-β signaling axis between tubules and fibroblasts in mice and humans. Even a single PDGF-B-expressing injured tubular cell could drive fibrogenesis by induction of a surrounding peritubular interstitial profibrotic niche. Despite PDGF-B being expressed or stored in kidney mesenchymal cells or megakaryocytes and platelets, *Pdgfb* deletion in these cells had no effect on healthy or fibrotic kidney models.

Conclusions: Paracrine PDGF signaling represents a key molecular mechanism of cellular crosstalk mediating the transition of kidney tubular injury to interstitial fibrosis.

Kidney International (2026) **109,** 1239–1255; https://doi.org/10.1016/j.kint.2026.01.029

KEYWORDS: cell-specific knockout; Cre; Cxcl4; Foxd1; Pax8

Copyright © 2026, International Society of Nephrology. Published by Elsevier Inc. This is an open access article under the CC BY license (http://creativecommons.org/licenses/by/4.0/).

Translational Statement

Kidney fibrosis is the underlying pathologic process of chronic kidney disease. Using gene expression analysis in mice and humans and several cell-specific transgenic mouse models, we identified paracrine platelet-derived growth factor (PDGF) signaling as a pivotal molecular mechanism of the transition of kidney tubular injury to interstitial fibrosis. We found a specific subset of injured tubular epithelial cells producing PDGF-B to be a critical mediator of fibrosis by orchestrating the activity of PDGF receptor-β^+ peritubular fibroblasts. This interaction fostered the formation of injury-associated profibrotic niches, highlighting the cellular dynamics involved in renal injury responses. These data support the translational potential of targeting this molecular crosstalk as a potential therapeutic strategy.

Platelet-derived growth factor-B (PDGF-B) is a member of the PDGF family, which comprises 5 dimeric ligands and 3 dimeric tyrosine kinase receptors.[1] PDGF-B activates all 3 PDGF receptors (PDGFRs), αα, αβ, and ββ, expressed by mesenchymal cells, which in the healthy kidney comprise mesangial cells, fibroblasts, pericytes, and vascular smooth muscle cells.[1–3]

PDGF-B is an important regulator of vascular formation and kidney development by stimulating the proliferation and migration of mesangial cells, which are crucial for the

Correspondence: *Barbara Mara Klinkhammer or Peter Boor, Institute of Pathology, RWTH Aachen University Hospital, Pauwelsstrasse 30, 52074 Aachen, Germany. E-mail: bklinkhammer@ukaachen.de or pboor@ukaachen.de*

Received 27 June 2025; revised 23 December 2025; accepted 16 January 2026; published online 28 February 2026

integrity and functionality of the glomerular filtration barrier.[4,5] Mice with ubiquitous or endothelial-specific *Pdgfb* knockout do not form the glomerular mesangium and die early because of hemorrhages. This shows that PDGF-B is necessary for the recruitment and differentiation of pericytes, which are essential for the formation and stabilization of renal microvessels.[6–8]

In the adult kidney, PDGF-B is mainly expressed by endothelial cells and to a low extent by mesangial cells, podocytes, and some tubular cells, and becomes strongly upregulated under disease conditions.[9–11] Dysregulated PDGF-B signaling has been implicated in various kidney pathologies (e.g., increased PDGF-B has been closely associated with renal fibrosis, a common feature of progressive chronic kidney diseases). Mechanistically, it was shown that in cell culture, PDGF-B stimulates proliferation and profibrotic activation of kidney fibroblasts and mesangial cells.[2,12] *In vivo,* the infusion of PDGF-B in rats led to proliferation of mesangial cells and increased extracellular matrix deposition in rats.[13] *Vice versa,* different therapeutic approaches to inhibit PDGF-B–PDGFR signaling showed beneficial antifibrotic effects in experimental models of mesangioproliferative anti-Thy1.1 nephritis, focal segmental glomerulosclerosis, unilateral ureteral obstruction (UUO), and ischemia-reperfusion injury (IRI).[11,14,15]

The relevant cellular sources of PDGF-B in the above scenarios remain elusive. To understand the functional relevance of the cellular crosstalk, we investigated the expression of PDGF-B in healthy and fibrotic human and murine kidneys and generated and analyzed 3 transgenic mouse lines with cell-specific deletion of *Pdgfb* in kidney epithelial cells, mesenchymal cells, and platelets. Although the deletion of *Pdgfb* in platelets and mesenchymal cells did not affect healthy or diseased kidneys, the deletion in epithelial cells significantly reduced kidney fibrosis in different models of injury by modulation of the fibrogenic niche.

METHODS

Most of the methods, including Supplementary Tables S1 (antibodies) and S2 (primers), are available in detail as Supplementary Material.

Study design and animals

We generated 3 cell-specific knockout mouse lines (i.e., *Pf4Cre::Pdgfb*, *Foxd1Cre::Pdgfb*, and *Pax8Cre::Pdgfb*), by crossbreeding of $Pdgfb^{flox/flox}$ mice (B6.129P2-$Pdgfb^{tm2Cbet}$/J; Jackson Laboratories strain 017622) with Pf4-Cre mice (C57BL/6-Tg[Pf4-icre]Q3Rsko/J; Jackson Laboratories strain 008535), with FoxD1-Cre mice (B6;129S4-$Foxd1^{tm1[GFP/cre]Amc}$/J; Jackson Laboratories strain 012463), or with Pax8-Cre mice (B6.129P2[Cg]-$Pax8^{tm1.1[cre]Mbu}$/J; Jackson Laboratories strain 028196).[6,16–18] Because we had to use different breeding strategies for the mouse lines dependent on the insertion of the Cre recombinase, and in terms of animal welfare wanted to produce as little breeding surplus as possible, we compared the following genotypes: $Pf4Cre^{+}$ $Pdgfb^{flox/flox}$ (knockout [KO]) versus $Pf4Cre^{+}$ $Pdgfb^{+/+}$ (control) (for *Pf4Cre::Pdgfb*), $Foxd1Cre^{+}$ $Pdgfb^{flox/flox}$ (KO) versus $Foxd1Cre^{+}$ $Pdgfb^{+/+}$ or $Foxd1Cre^{-}$ $Pdgfb^{flox/+}$ or $Foxd1Cre^{-}$ $Pdgfb^{+/+}$ (control) (for *Foxd1Cre::Pdgfb*), and $Pax8Cre^{+}$ $Pdgfb^{flox/flox}$ (KO) versus $Pax8Cre^{-}$ $Pdgfb^{flox/flox}$ (control) (for *Pax8Cre::Pdgfb*). For ease of reading, we refer to each group in each section as KO versus control littermates. No animal died or had to be excluded in the course of the experiments. In total, we used 229 mice (120 males and 109 females) for cell isolation, analyses of spontaneous kidney phenotypes, and the cell-specific role of PDGF-B in kidney fibrosis models plus data from 43 male C57BL/6N mice from a previously published UUO time course study (Figure 1).[19,20]

Human kidney specimen

Human kidney formalin-fixed, paraffin-embedded samples were collected from biopsy specimens at the Institute of Pathology of the University Clinic RWTH Aachen. All samples were handled anonymously, and the study was approved by the local review board (EK244/14 and EK042/17) and in line with the Declaration of Helsinki. The following 4 patients were included for *PDGFB in situ* hybridization: female, 17 years, approximately 1% interstitial fibrosis and tubular atrophy; male, 68 years, transplant, approximately 1% interstitial fibrosis and tubular atrophy; male, 38 years, diabetic nephropathy, approximately 30% interstitial fibrosis and tubular atrophy; and male, 69 years, diabetic nephropathy, approximately 30% interstitial fibrosis and tubular atrophy.

Renal morphology and quantitative digital pathology

Kidney tissues for histopathologic analyses were fixed in methyl Carnoy solution or formalin and embedded in paraffin. Sections of 1 μm were cut with a microtome and stained with periodic acid–Schiff and counterstained with hematoxylin for overall assessment of kidney morphology and damage (blinded manner).

Periodic acid–Schiff–stained slides from all experiments were also digitized, followed by automated multiclass segmentation and quantitative analysis using our recently published automated deep-learning–based approach.[21,22] Results were analyzed in R using our recently published tRigon package.[23]

Statistical analysis

The sample size of each group comprised at least 3 animals or cell samples. All statistical analyses were performed using GraphPad Prism 9.3.1. Data are presented as individual values plus additional indication of mean ± SD or as violin plots plus additional box plots to show distributions. Data were tested for normal distribution (D'Agostino-Pearson and Kolmogorov-Smirnov), and appropriate statistical tests were used for comparisons: for 2 groups the 2-tailed unpaired Student *t* test or Mann-Whitney; and for >2 groups, 1-way

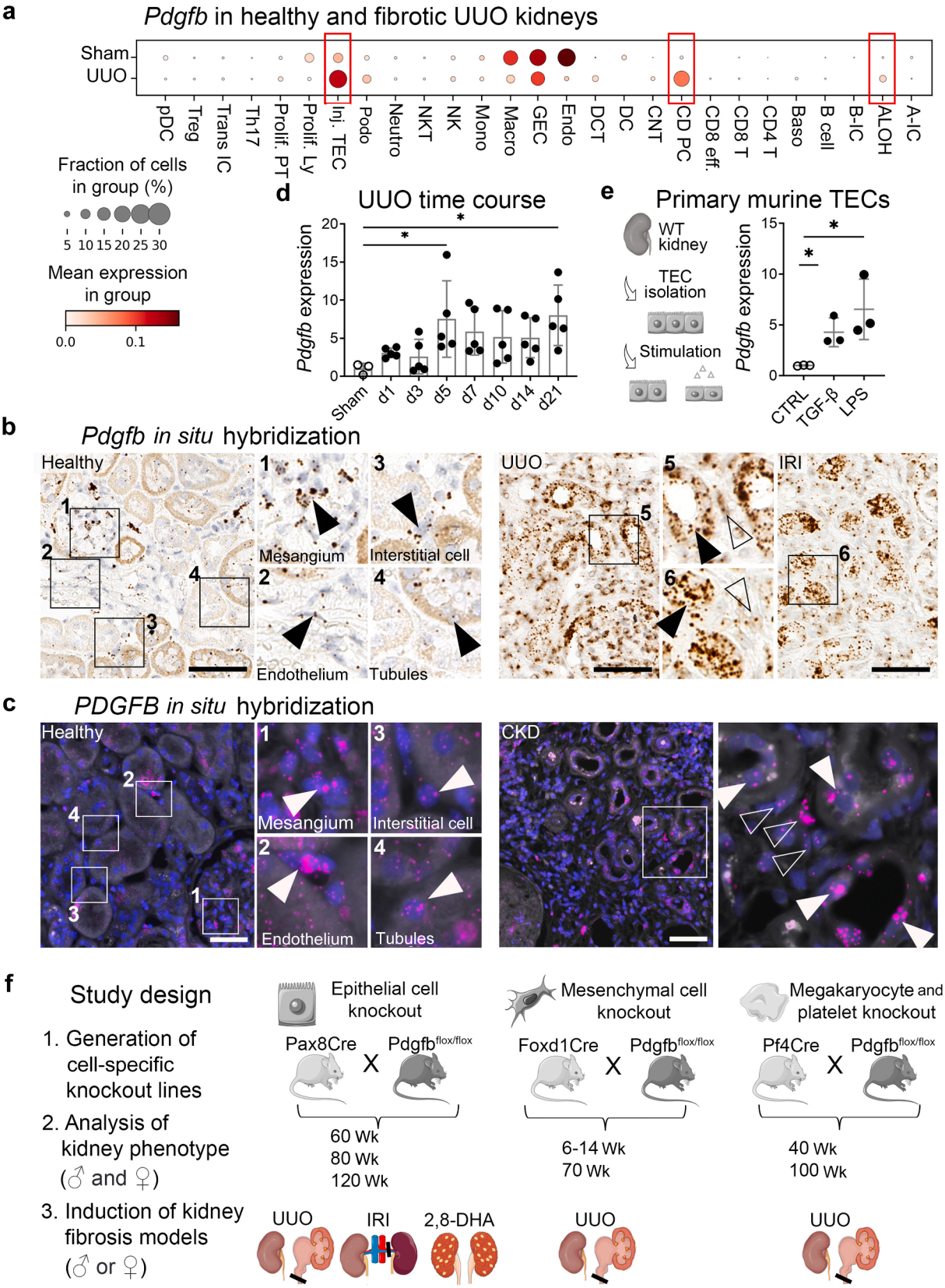


Figure 1 | Platelet-derived growth factor-B (PDGF-B) expression in murine kidneys and cell-specific knockout mice. (**a**) Analyses of single-cell *Pdgfb* expression in a mouse unilateral ureteral obstruction (UUO) model. Red boxes mark epithelial cell populations with upregulated expression. (**b**) Brown *in situ* hybridization depicts *Pdgfb* expression in histologic samples from murine UUO and ischemia-reperfusion injury (IRI) models. Healthy: black arrows mark *Pdgfb* expression in mesangial cells, interstitial cells, endothelium, (continued)

analysis of variance with Tukey *post hoc* test or Kruskal-Wallis test were used for normal and not-normally distributed data, respectively. Statistical significance was defined as $P < 0.05$.

RESULTS

PDGF-B is upregulated in kidney disease

We reanalyzed kidney expression of murine *Pdgfb* and human *PDGFB* in publicly available single-cell RNA-sequencing datasets.[24,25] In healthy murine and human kidneys, *Pdgfb*/*PDGFB* expression was most prominent in endothelial cells from vessels of different calibers and resident macrophages, and lower to negligible expression was found in various tubular segments (Figure 1a and Supplementary Figure S1). We confirmed this by *in situ* hybridization, which revealed strong *Pdgfb*/*PDGFB* expression in healthy nonfibrotic kidneys in mesangial cells and endothelium, and low expression in interstitial cells and tubules (Figure 1b and c).

In diseased kidneys, *Pdgfb* was highly and significantly upregulated (Figure 1b and d). In 2 models of kidney fibrosis (i.e., UUO and ischemia-reperfusion injury), there was a progressive upregulation confirmed by quantitative reverse transcription–polymerase chain reaction and *in situ* hybridization (Figure 1b and d). Both human and mouse data indicated that epithelial cells and interstitial pericytes exhibited increased *PDGFB* expression in fibrosis (Figure 1a–c and Supplementary Figure S1). *In vitro,* treatment of primary murine cortical tubular cells with the profibrotic transforming growth factor-β or proinflammatory lipopolysaccharide induced *Pdgfb* expression (Figure 1e).

These data and previous findings[4,8,11,26] suggested endothelial, epithelial, or mesenchymal cells as potential intrarenal sources of PDGF-B. Additionally, platelets represent a major extrarenal source (hence the name "platelet-derived growth factor").[27] To understand the role of *Pdgfb* from these specific cells, we generated 3 transgenic mouse lines (i.e., *Pax8Cre::Pdgfb, Foxd1Cre::Pdgfb, and Pf4Cre::Pdgfb*) lacking *Pdgfb* in kidney epithelial cells, kidney mesenchymal cells, or megakaryocytes and platelets, respectively (Figure 1f). Mice with endothelial-specific deletion of *Pdgfb* were shown to have serious developmental defects, including cardiac, kidney, and brain abnormalities, and were therefore not used.[8,28]

Deletion of PDGF-B in kidney epithelial cells reduces kidney mesenchyme

We generated *Pax8Cre::Pdgfb*$^{flox/flox}$ mice, lacking *Pdgfb* in kidney epithelial cells, including tubular cells, podocytes, and parietal epithelial cells, as shown by polymerase chain reaction and *in situ* hybridization (Figure 2a and b, black arrows). Tubular *Pdgfb* deletion did not affect kidney function, but the transgenic male and female mice, aged 60, 80, or 120 weeks, exhibited significantly smaller kidneys compared with control littermates (Figure 2c–f, Supplementary Figure S2, and Supplementary Tables S3–S5). The kidney morphology appeared inconspicuous, but a deep-learning–based tissue segmentation and analysis of derived features (i.e., pathomics) revealed a significantly smaller medullary interstitium (Figure 2g and Table 1). We confirmed this by immunostainings showing a reduced expression of PDGFR-β and collagen III, particularly in the medulla (Figure 2h and i). We performed bulk RNA sequencing and performed analysis of relevant signaling pathways using PROGENy.[29] This demonstrated the PDGFR downstream pathways mitogen-activated protein kinase and phosphatidylinositol-3′-kinase to be reduced in *Pax8Cre::Pdgfb*$^{-/-}$ KO mice compared with control mice (Figure 2j).

In summary, kidneys with a constitutive deletion of *Pdgfb* in kidney epithelial cells have a normal function even in high age, despite slight structural alterations, particularly reduced medullary interstitial cells, and matrix.

Epithelium-derived PDGF-B drives kidney fibrosis

Next, we subjected these mice to different kidney fibrosis models. Five days after UUO, transgenic *Pax8Cre::Pdgfb* KO mice had significantly lower *Pdgfb* mRNA and PDGF-BB protein expression compared with control littermates, suggesting epithelial *Pdgfb* as a major source of *de novo* expressed renal *Pdgfb* during fibrosis (Figure 3a–d). Quantification of *Pdgfb in situ* hybridization confirmed a specific KO in the tubules, whereas there was no significant difference in the *Pdgfb* expression in the interstitium (Supplementary Figure S3). PDGFR-β immunostaining revealed a significantly lower protein expression, in line with a significant decrease in α-smooth muscle actin (α-SMA) staining, reflecting a lower number of interstitial (myo)fibroblasts (Figure 3f and g). Consistently, the KO mice had a significantly lower expression of collagen III (Figure 3h). There was no change in the expression of *Pdgfd*, the other

Figure 1 | (continued) and tubules. UUO and IRI: black arrows mark *Pdgfb* expression in tubules, and transparent arrows mark Pdgfb expression in interstitial cells. (**c**) Magenta fluorescence *in situ* hybridization depicts *PDGFB* expression in histologic samples from human patient biopsy samples. (**d**) Quantitative reverse transcription–polymerase chain reaction analysis confirms a significant upregulation of *Pdgfb* in a time course of the murine UUO model. (**e**) *Pdgfb* regulation in cultured primary murine tubular epithelial cells after stimulation with profibrotic transforming growth factor (TGF)–β or proinflammatory lipopolysaccharide (LPS). (**f**) Design of the current study involving 3 different cell-specific *Pdgfb* knockout mouse lines. Bar = 50 μm. 2,8-DHA, 2,8-dihydroxyadenine; A-IC, α intercalated cell; ALOH, ascending limb of Loop of Henle; Baso, basophil; B-IC, β intercalated cell; CD8 eff., effector CD8$^+$ T cells; CD PC, collecting duct principal cell; CKD, chronic kidney disease; CNT, connecting tubule; CTRL, control; d, day; DC, dendritic cell; DCT, distal convoluted tubule; Endo, endothelial cell; GEC, glomerular endothelial cell; Inj. TEC, injured tubular epithelial cell; Macro, macrophage; Mono, monocyte; Neutro, neutrophil; NK, natural killer cell; NKT, natural killer T cell; pDC, plasmacytoid dendritic cell; Podo, podocyte; Prolif. Ly, proliferating lymphocyte; Prolif. PT, proliferating proximal tubule cell; TEC, tubular epithelial cell; Th17, T_H17 subset of helper T; Trans IC, transitional intercalated cell; Treg, regulatory T cell; WT, wild type. To optimize viewing of this image, please see the online version of this article at www.kidney-international.org.

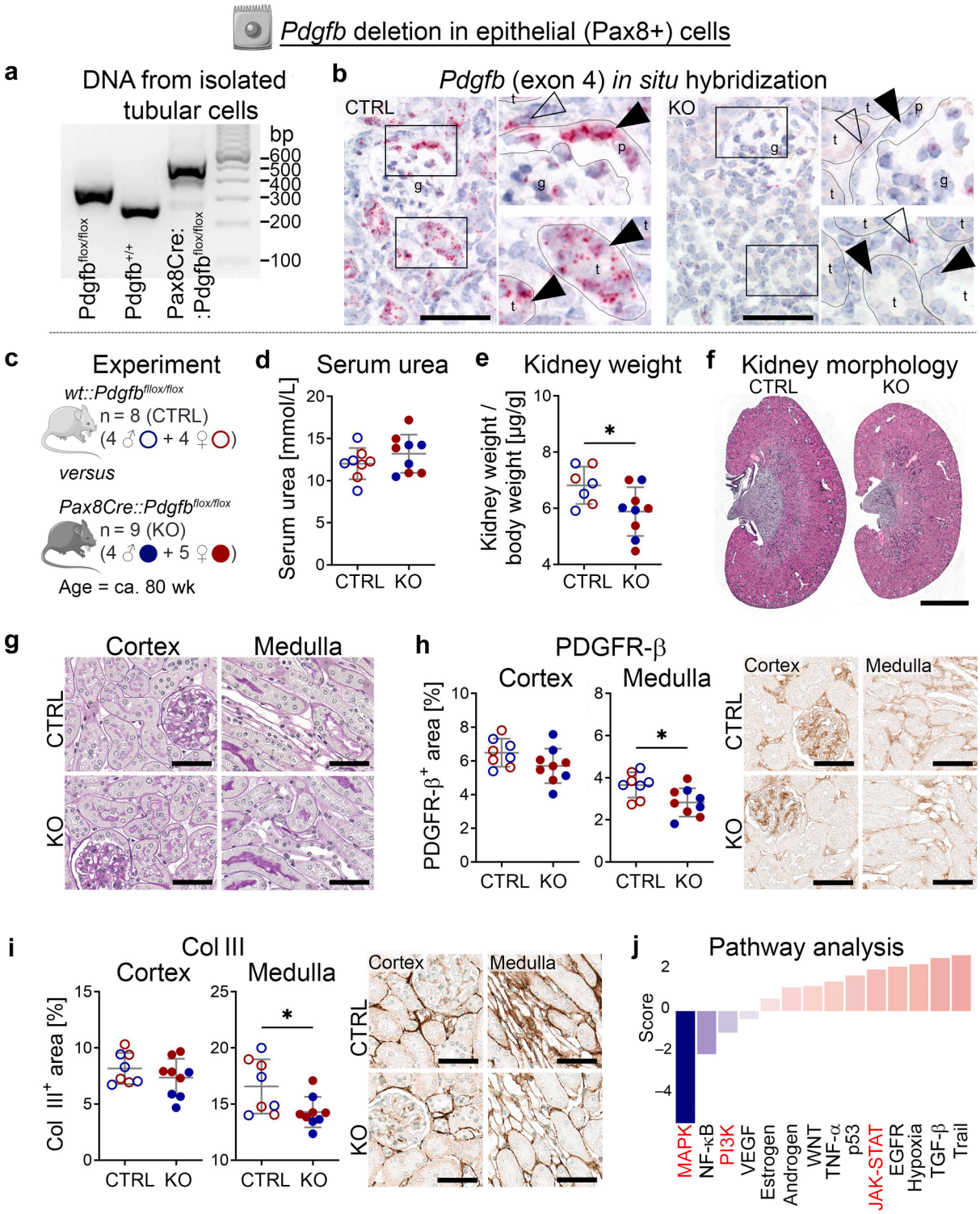


Figure 2 | Spontaneous phenotype in *Pax8Cre::Pdgfb* mice. (**a**) Polymerase chain reaction with genomic DNA isolated from primary tubular epithelial cells confirms the deletion of platelet-derived growth factor-B (PDGF-B) in platelets. (**b**) Red *in situ* hybridization depicts *Pdgfb* expression in histologic samples from wild-type–like control (CTRL) mice and mice with epithelial cell–specific *Pdgfb* deletion (knockout [KO]) of the *Pax8Cre::Pdgfb* line after unilateral ureteral obstruction. For better visualization, structures are outlined in the close-up images. (**c**) Experimental design. At the age of 80 weeks, 8 CTRL animals were compared with 9 KO mice. Males are shown in blue, and females are shown in red. (**d**) Serum urea. Kidneys from KO mice are (**e**) lighter and smaller, as shown by (**f**) histologic silver-stained cross-sections. (**g**) Although periodic acid–Schiff stains do not show any clear pathologic signs, immunostainings for (**h**) PDGF receptor (PDGFR)–β and (**i**) collagen (Col) type III confirm a significant reduction of expression in the medulla. (**j**) Pathway analysis (PROGENy) in bulk RNA-sequencing data from 4 male wild-type–like control (CTRL) versus 4 male mice with epithelial-specific Pdgfb deletion (KO). Known PDGFR downstream pathways are marked in red. *$P < 0.05$ (unpaired *t* test or Mann-Whitney). Bar = 50 µm. Arrow indicates epithelial cell; and blank arrow, (continued)

Table 1 | Quantitative morphologic analyses after automated segmentation of PAS-stained sections (pathomics) of *Pax8Cre::Pdgfb*$^{flox/flox}$ mice

	Pax8Cre::Pdgfb female mice		*Pax8Cre::Pdgfb* male mice	
Variable	WT (n = 4)	KO (n = 5)	WT (n = 4)	KO (n = 4)
Interstitium (cortex), %	25.1 ± 3.2	27.5 ± 1.0	29.0 ± 2.1[a]	27.8 ± 2.4
Interstitium (medulla), %	39.1 ± 2.5	37.2 ± 2.9	43.4 ± 2.0	39.1 ± 1.3[b]
No. of tubule cross-sections (cortex)	32,238	39,198	36,715	30,602
No. of tubule cross-sections (medulla)	50,754	64,489	52,175	46,162
Tubule size (cortex), μm^2	1000 ± 940	997 ± 852[b]	1392 ± 1329[a]	1414 ± 1236[a,b]
Tubule size (medulla), μm^2	849 ± 1322	978 ± 2308[b]	929 ± 1077[a]	980 ± 1035[a,b]
Tubule diameter (cortex), μm	23.2 ± 7.2	23.7 ± 6.9[b]	26.8 ± 8.9[a]	27.3 ± 8.8[a,b]
Tubule diameter (medulla), μm	19.4 ± 8.6	20.8 ± 9.4[b]	19.9 ± 7.4[a]	21.7 ± 7.6[a,b]
No. of glomerular cross-sections	877	1,211	849	793
Glomerular size (area), μm^2	3513 ± 1609	3462 ± 1606	4595 ± 2183[a]	4146 ± 1894[a,b]
Glomerular diameter, μm	56.8 ± 14.4	56.8 ± 15.1	65.0 ± 17.3[a]	61.9 ± 15.8[a,b]
Glomerular circularity	0.81 ± 0.1	0.82 ± 0.09	0.8 ± 0.12	0.81 ± 0.09
Tuft size (area), μm^2	2459 ± 1334	2503 ± 1403	2874 ± 1794	2696 ± 1615
Tuft diameter, μm	45.2 ± 14.4	45.7 ± 15.5	48.5 ± 16.4[a]	47.6 ± 16.3[a]
Tuft circularity	0.69 ± 0.11	0.7 ± 0.1[b]	0.66 ± 0.11[a]	0.67 ± 0.11[a,b]
Bowman's capsule (area), μm^2	1054 ± 704	959 ± 453	1720 ± 900[a]	1449 ± 754[a,b]

KO, knockout; PAS, periodic acid–Schiff; WT, wild type.
[a]$P < 0.05$ female versus male (same genotype).
[b]$P < 0.05$ KO versus WT.
Data are shown as mean ± SD unless otherwise specified.

ligand for PDGFR-β, suggesting that the effects were mediated via the PDGF-B–PDGFR-β axis (Figure 3e). There were no differences in kidney function, lipocalin-2 expression, cell death, or inflammation, as indicated by similar amounts of CD45 and F4/80 positively stained area and similar expression of profibrotic (M1) macrophage markers *Cd86* and interleukin-6 (*Il6*) and prorepair (M2) macrophage markers mannose receptor, C type 1 (*Mrc1*), and *Il10* (Figure 3i and j and Supplementary Figure S4). We confirmed these data in a second mouse model, the unilateral ischemia-reperfusion injury. On day 21, the KO mice exhibited reduced fibrosis, as shown by significantly lower PDGFR-β, α-SMA, and collagen III expression in the cortex, whereas there was no difference in kidney function, lipocalin-2, cell death, and inflammation (CD45, F4/80, *Cd86*, *Il6*, *Mrc*, and *Il10*) compared with control littermates (Figure 3k–r and Supplementary Figure S5).

In a third model of crystal-induced injury, the 2,8-dihydroxyadenine nephropathy, we also found significantly reduced fibrosis in the kidney cortex on day 21 of the 2,8-dihydroxyadenine model in *Pax8Cre::Pdgfb*$^{-/-}$ KO mice, analyzed by PDGFR-β, α-SMA, and collagen III expression in cortex. There were no significant differences in body weight, kidney weight, blood pressure, serum urea, serum cystatin C, serum creatinine, or creatinine clearance between KO and control littermates (Figure 4a–j and Supplementary Figure 6A and B). Interestingly, and in contrast to both unilateral models, we found significantly increased tubular injury analyzed by lipocalin-2 expression analysis in the cortex of KO mice. Similar to the other models, cell death and inflammation were similar in both groups (Figure 4k–m and Supplementary Figure 6C–I).

Epithelium-derived PDGF-B shapes profibrotic niches in kidney fibrosis

To further elucidate the mechanism of reduced fibrosis after epithelial PDGF-B deletion, we costained *Pdgfb* and *Pdgfrb* by *in situ* hybridization on sections from UUO day 5 control mice. This revealed interstitial *Pdgfrb*$^+$ cells (magenta) in close proximity to tubular cells expressing high levels of *Pdgfb* (green) (Figure 5a). In some tubules, we found single isolated *Pdgfb*$^+$ epithelial cells in 1 tubule cross-section, which were surrounded by peritubular *Pdgfrb*$^+$ cells, suggesting paracrine PDGF-mediated signaling between epithelial cells and interstitial cells that can be induced by 1 single injured tubular cell (Figure 5a). These peritubular *Pdgfrb*$^+$ cells also expressed other mesenchymal (profibrotic) markers, like α-SMA, transgelin, and the extracellular matrix (ECM) proteins tenascin C (TNC) and periostin (*Postn*) (Figure 5b). The *Pdgfb*$^+$ tubular cells often also expressed *Clcf1*, a recently identified marker for persistently injured tubules and involved in an interplay between tubular cells

Figure 2 | (continued) interstitial cell. EGFR, epidermal growth factor receptor; g, glomerular tuft; JAK, Janus kinase; MAPK, mitogen-activated protein kinase; NF-κB, nuclear factor-κB; p, parietal epithelial cell; PI3K, phosphatidylinositol-3′-kinase; STAT, signal transducer and activator of transcription; t, tubule; TGF-β, transforming growth factor-β; TNF-α, tumor necrosis factor-α; Trail, xxx; VEGF, vascular endothelial growth factor; WNT, xxx. To optimize viewing of this image, please see the online version of this article at www.kidney-international.org.

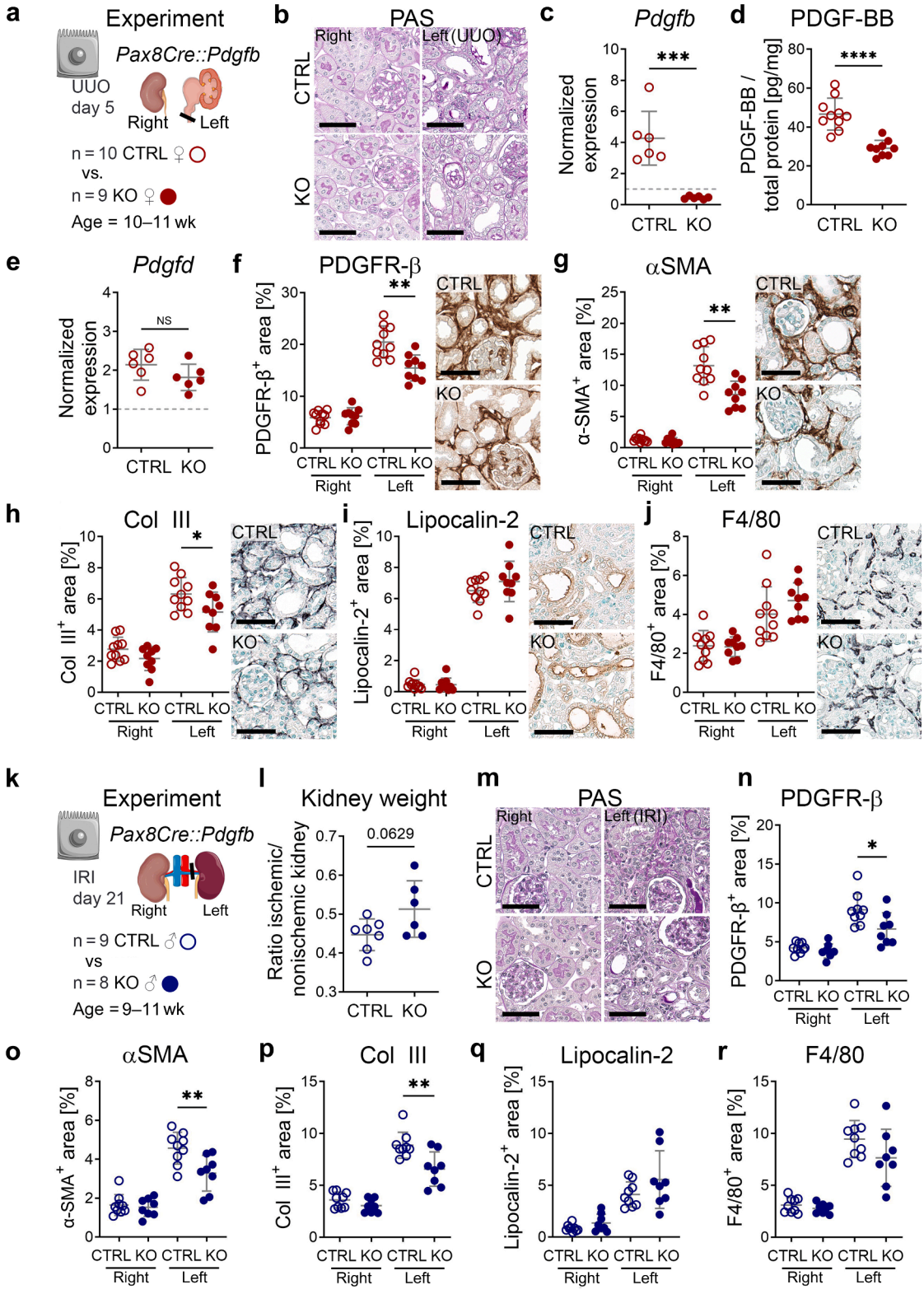


Figure 3 | Unilateral ureteral obstruction (UUO) and ischemia-reperfusion injury (IRI) in *Pax8Cre::Pdgfb* mice. (**a**) Experimental design of the UUO experiment. At the age of 10 to 11 weeks, kidney cortex of 10 wild-type–like control (CTRL) animals was compared with cortex of 9 mice with *Pdgfb* deletion specifically in epithelial Pax8-positive cells (knockout [KO]). Females are shown in red. (**b**) Periodic acid–Schiff (PAS)–stained kidney histology does not show any abnormalities in the KO mice. On (**c**) mRNA and (**d**) protein level, *Pdgfb*/platelet-derived growth factor-B (PDGF-B) is significantly reduced in the cortex of KO mice, whereas (**e**) *Pdgfd* is not. For technical reasons, the number of animals in the *Pdfgb* and *Pdfgd* polymerase chain reaction analysis was reduced to 6 per group. Immunostainings reveal a significant reduction of (**f**) platelet-derived growth factor receptor (PDGFR)–β, (**g**) α-smooth muscle actin (α-SMA), and (**h**) collagen (Col) type III, whereas (continued)

and interstitial fibroblasts in acute kidney injury–chronic kidney disease transition (Figure 5b).[30]

We found a matching expression pattern for *PDGFB* and *PDGFRB* in human fibrotic kidney sections (Figure 5c). Analysis of cell-cell interactions in the human Kidney Precision Medicine Project dataset confirmed an increased interaction of $PDGFB^+$ proximal tubules (PTs) and $PDGFRB^+$ fibroblasts in chronic kidney disease, whereas there was no interaction between $PDGFB^-$ PTs and $PDGFRB^+$ or $PDGFRB^-$ fibroblasts (Figure 5d). $PDGFB^-$ PTs expressed genes related to cell metabolism, and the top upregulated genes included mostly proteins that are typically expressed by epithelial cells (e.g., intracellular or solute transporters) (Supplementary Figure S7A–C). $PDGFB^+$ PTs expressed genes that are important for tissue/cell morphogenesis and cell motility and migration (Supplementary Figure S7A). Among the top upregulated genes in the $PDGFB^+$ PTs were ECM proteins and integrins (Supplementary Figure S7B and D). Ligand-receptor interaction scores revealed that 10 of the top 50 interactions between $PDGFB^+$ PTs and $PDGFRB^+$ fibroblasts are mediated via ECM-integrin binding and *vice versa* even 13 of the top 50 (e.g., by fibroblast-derived tenascin C) (Supplementary Tables S6 and S7). A transcription factor analysis showed that $PDGFB^+$ PTs generally exhibit higher activity than $PDGFB^-$ PTs (Supplementary Figure S7E). The 2 factors with most differential activity (i.e., forkhead box A2 [*FOXA2*] and TEA domain family member 1 [*TEAD4*]) have been identified as regulators of hepatitis A virus cellular receptor 1 (HAVCR1; kidney injury molecule-1 [Kim-1]).[31–33] Among the top 20 transcription factors were at least 8 (i.e., forkhead box protein O1 [*FOXO1*], homeobox protein Hox-B13 [*HOXB13*], glucocorticoid receptor [*NR3C1*], CCAAT/enhancer-binding protein β [*CEBPB*], Fos-related antigen 1 [*FOSL1*], *FOSL2*, *TEAD1*, and activating transcription factor 3 [*ATF3*]) that were predicted or experimentally shown to regulate *PDGFB* transcription.

In UUO day 5 kidneys of the *Pax8Cre::Pdgfb* KO mice, we found a reduced expression of doublecortin domain-containing 2 (Figure 6a). Doublecortin domain-containing 2 was 1 of the top upregulated genes in human $PDGFB^+$ tubules (Supplementary Figure 7D) and was previously described to be expressed by maladaptive PTs after failed repair.[25,34] We also found Kim-1, another marker of this tubule population in the fibrotic microenvironment,[34,35] to be reduced in the *Pax8Cre::Pdgfb* KO mice, matching the transcription factor analysis in human samples (Figure 6b and Supplementary Figure S8). In line with this, Gene Ontology enrichment analysis of the bulk RNA data from *Pax8Cre::Pdgfb* KO mice with UUO showed that downregulated gene sets were mainly involved in energy metabolism and mitochondrial activity, whereas genes involved in epithelial cell proliferation, migration, adhesion, and inflammatory cytokine production were activated (Supplementary Figure S7F). The analysis of mesenchymal cell proliferation using PDGFR-β + Ki-67 costaining revealed a significantly reduced proliferation in the PDGFR-β^+ interstitial cells in *Pax8Cre::Pdgfb* KO mice (Figure 6c).

Taken together, the deletion of *Pdgfb* in epithelial cells significantly reduced kidney fibrosis, via diminished paracrine signaling between tubular epithelium and neighboring interstitial cells and reduced formation of fibrotic niches.

Autocrine PDGF-B signaling in kidney mesenchymal cells does not affect kidneys

Given the upregulation of PDGF-B in kidney mesenchymal cells in fibrosis, we next examined the potential autocrine role of PDGF-B in these cells. *Foxd1Cre::Pdgfb* KO mice lacked expression of *Pdgfb* in kidney mesenchymal cells, but not in tubules, as shown by *in situ* hybridization (Figure 7a and Supplementary Figure S9). The mice developed normally without any abnormalities in blood counts, blood pressure, body weight, kidney function, or kidney morphology at young (6–14 weeks) or older (70 weeks) ages (Supplementary Tables S8 and S9 and Supplementary Figure S10).

In the UUO model, KO mice showed no significant changes in kidney pathology (periodic acid–Schiff), inflammation, or fibrosis analyzed by immunostainings for PDGFR-β and α-SMA, collagen III, and F4/80 (Figure 7b, c, and f–j). The lack of *Pdfgb* expression specifically in the kidney mesenchyme had no significant effect on the total *Pdgfb* expression and PDGF-BB concentration measured in the whole kidney cortex, potentially reflecting relatively low amounts of PDGF-B derived from mesenchymal cells (Figure 7d and e). The expression of PDGFR-β on mRNA level significantly increased, which, however, did not translate to changes on protein level, confirming similar amounts of activated fibroblasts between the groups (Figure 7f and g).

Taken together, constitutive deletion of *Pdgfb* in mesenchymal cells did not exert relevant effects on the healthy or fibrotic kidneys.

Platelet-derived PDGF-B does not affect healthy or diseased kidneys

Because PDGF is stored in platelets, and platelets are involved in wound healing, we analyzed the impact of

Figure 3 | (continued) (**i**) lipocalin-2 and (**j**) F4/80 are similarly expressed in both groups. (**k**) Experimental design of the IRI experiment. At the age of 9 to 11 weeks, 9 male CTRL animals are compared with 8 male KO mice (both cortex). (**l**) Ratio of kidney weights from ischemic left kidney to nonischemic right kidney reveals lower organ shrinkage after IRI in the KO mice. (**m**) PAS-stained kidney histology does not show any abnormalities in the KO mice. Similar to the UUO model, immunostainings reveal a significant reduction of (**n**) PDGFR-β, (**o**) α-SMA, and (**p**) Col type III, whereas (**q**) lipocalin-2 and (**r**) F4/80 are similarly expressed in both groups. $^*P < 0.05$, $^{**}P < 0.01$, $^{***}P < 0.001$ (analysis of variance or Kruskal-Wallis, or unpaired *t* test or Mann-Whitney, respectively). NS, not significant. Bar = 50 μm. To optimize viewing of this image, please see the online version of this article at www.kidney-international.org.

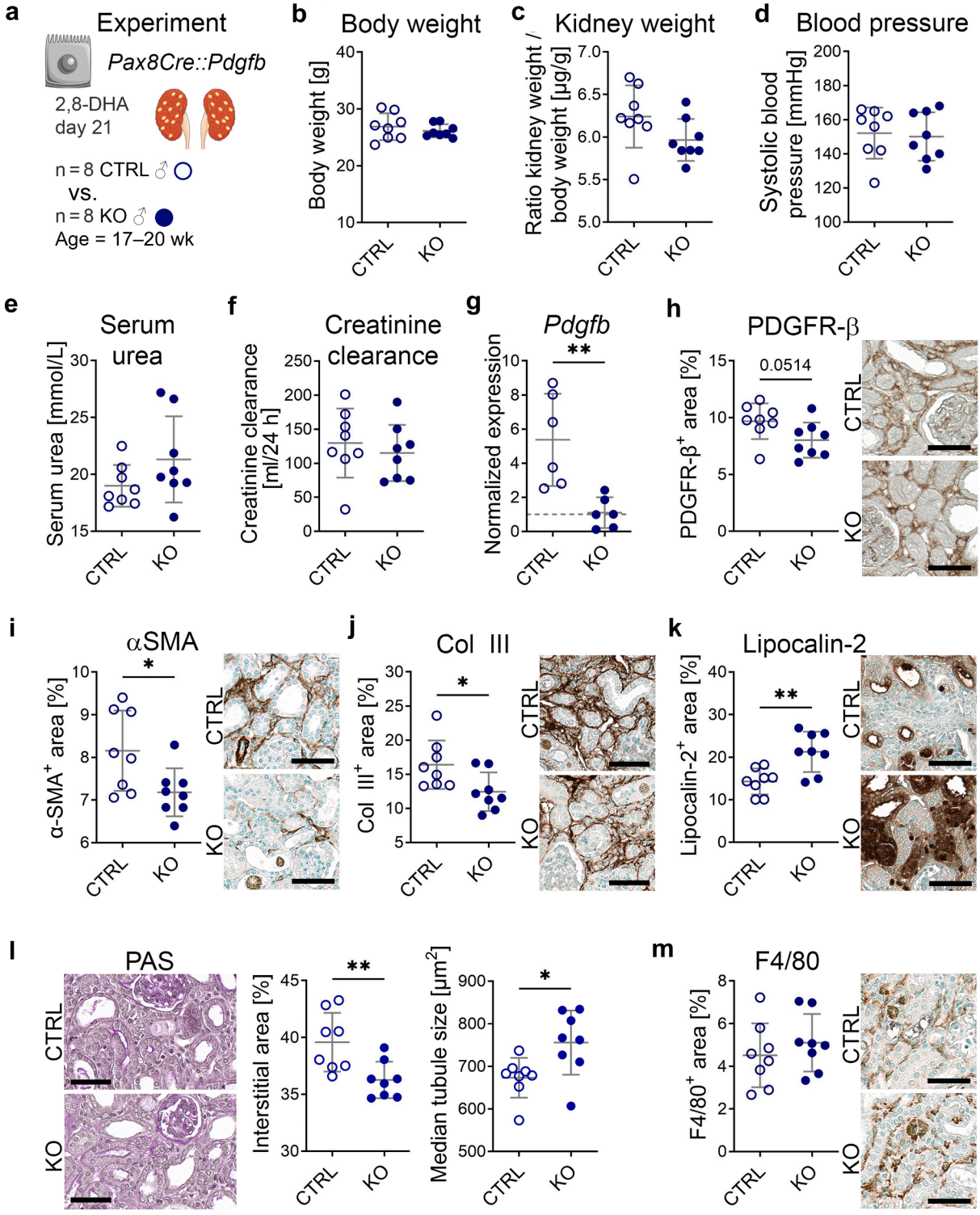


Figure 4 | 2,8-Dihydroxyadenine (2,8-DHA) nephropathy in *Pax8Cre::Pdgfb* mice. (**a**) Experimental design. At the age of 17 to 20 weeks, male mice are fed with an adenine-enriched diet for 21 days. Eight wild-type–like control (CTRL) males were compared with 8 mice with epithelial-specific platelet-derived growth factor-b (Pdgfb) deletion (knockout [KO]). There are no differences between the groups for (**b**) body weight, (**c**) kidney weight, (**d**) systolic blood pressure, (**e**) serum urea, or (**f**) creatinine clearance. (**g**) Pdgfb mRNA expression is reduced in the KO mice, whereas (**h**) platelet-derived growth factor receptor (PDGFR)–β expression in cortex analyzed by immunostaining only shows a trend. Immunostainings for (**i**) α-smooth muscle actin (α-SMA) and (**j**) collagen (Col) type III reveal a significantly reduced expression in the cortex of KO mice, whereas (**k**) lipocalin-2 is significantly increased. (**l**) Automatically segmented periodic acid–Schiff (PAS)–stained kidney histology shows a reduced interstitium but larger tubular cross-sections (shown by violin distribution, n[tubules]: CTRL = 53,119; KO = 55,204). (**m**) F4/80 expression in cortex is similar between both groups. *$P < 0.05$, **$P < 0.01$ (unpaired *t* test or Mann-Whitney). Bar = 100 µm. To optimize viewing of this image, please see the online version of this article at www.kidney-international.org.

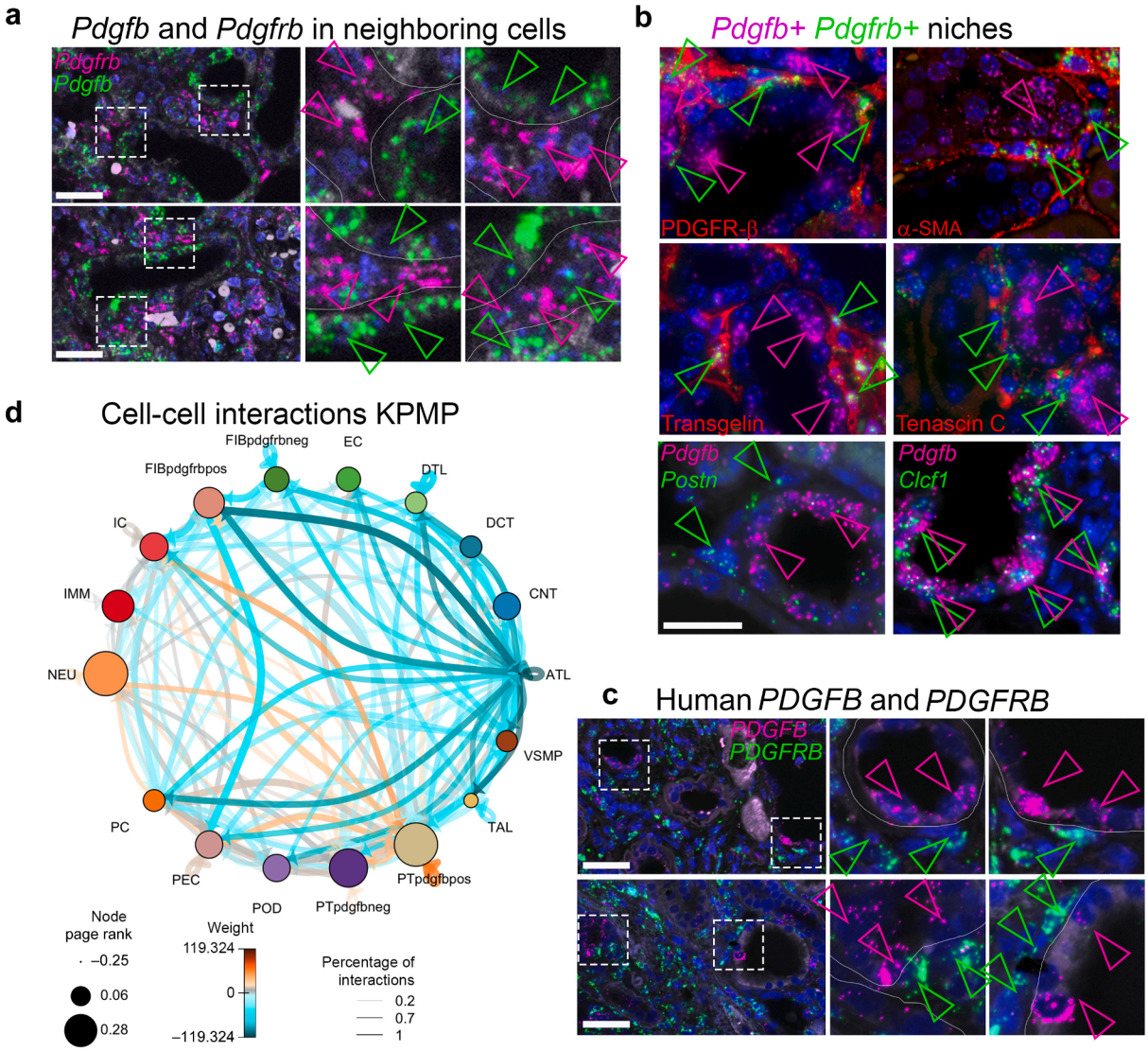


Figure 5 | Analysis of platelet-derived growth factor-B (PDGF-B)–PDGF receptor (PDGFR)–β axis. (**a**) Fluorescence *in situ* hybridization to detect *Pdgfb* (green) and its receptor *Pdgfrb* (magenta) in control (CTRL) mice with day 5 unilateral ureteral obstruction (UUO). For better visualization, structures are outlined in the close-up images. (**b**) Fluorescence *in situ* hybridization for *Pdgfb* (magenta) and *Pdgfrb* (green) in combination with immunostains (red) for PDGFR-β, α-smooth muscle actin (α-SMA), transgelin, and tenascin C in CTRL mice with day 5 UUO. Lower panel shows cofluorescence *in situ* hybridization for *Pdgfb* (magenta) and *Postn* or *Clcf1* (red) in CTRL mice with day 5 UUO. (**c**) Fluorescence *in situ* hybridization for *PDGFB* (magenta) and *PDGFRB* (green) in fibrotic human kidneys. (**d**) Cell-cell interactions in chronic kidney disease versus healthy kidneys based on single-cell RNA-sequencing data from the Kidney Precision Medicine Project (KPMP). Bar = 25 μm. ATL, ascending thin limb; CNT, connecting tubule; DCT, distal convoluted tubule; DTL, descending thin limb; EC, endothelial cell; FIBpdgfrbneg, fibroblasts without PDGFR-β; FIBpdgfrbpos, fibroblasts with PDGFR-β; IC, intercalated cell; IMM, immune cell; NEU, neural cell; PC, principal cell; PEC, parietal epithelial cell; POD, podocyte; PTpdgfbneg, proximal tubules without PDGF-B; PTpdgfbpos, proximal tubules with PDGF-B; TAL, thick ascending limb; VSMP, vascular smooth muscle cell or pericyte. To optimize viewing of this image, please see the online version of this article at www.kidney-international.org.

platelet-derived PDGF-B in healthy and fibrotic kidneys. *Pf4Cre:Pdgfb* KO mice lacked expression of PDGF in platelets, as confirmed by Western blot in platelet lysates (Figure 8a). The mice developed normally and showed similar *Pdgfb* mRNA expression in kidneys as wild-type littermates (Supplementary Figure S11A). At 40 and 100 weeks of age, the mice showed slight changes in blood counts (i.e., higher hemoglobin and hematocrit and a shift toward a higher proportion of neutrophils) (Supplementary Tables S10 and S11). However, no difference in blood pressure, body weight, or kidney function and morphology could be observed (Supplementary Figure S11B–K). Although the healthy KO animals showed significantly less collagen expression in the kidney cortex (Supplementary Figure 11J), pathomics revealed a similar interstitial area (Supplementary Table S12). We did not find any effects of platelet-specific PDGF-B deficiency on fibrosis in the UUO model (Figure 8b and c). The KO in platelets also did not affect kidney expression of the *Pdgfb* mRNA; however, there was significantly less PDGF-BB protein detectable (Figure 8d

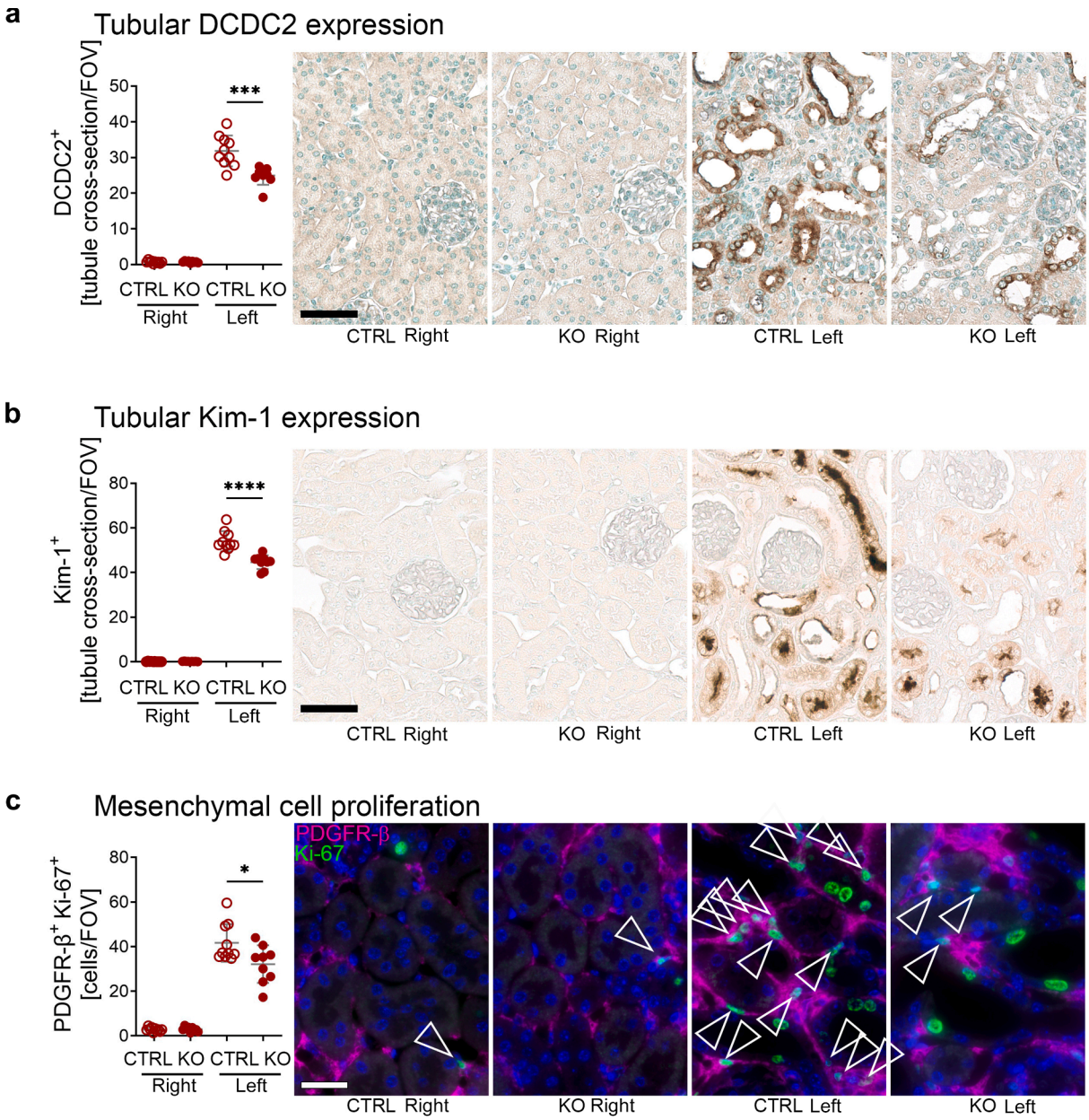


Figure 6 | Cellular characterization of *Pax8Cre::Pdgfb* mice on unilateral ureteral obstruction day 5 (UUOd5). (**a**) Quantification and representative images of doublecortin domain-containing 2 (DCDC2)–positive tubules. (**b**) Quantification and representative images of kidney injury molecule-1 (Kim-1; hepatitis A virus cellular receptor 1 [Havcr])–positive tubules. (**c**) Quantification of proliferating kidney mesenchymal cells in UUOd5 kidneys of control (CTRL) and knockout (KO) mice. Double-positive cells (arrowheads) were counted in kidney cortex in immunofluorescence stainings for Ki-67 (green) and platelet-derived growth factor receptor (PDGFR)–β (magenta). Bars = 50 μm. FOV, field of view. To optimize viewing of this image, please see the online version of this article at www.kidney-international.org.

and e). There was no difference in the accumulation of activated fibroblasts (PDGFR-β and α-SMA), collagen deposition, or infiltration of F4/80$^+$ immune cells (Figure 8f–j).

Taken together, constitutive deletion of *Pdgfb* in platelets did not exert relevant effects on the healthy or fibrotic kidneys.

DISCUSSION

In this study, we showed that the cellular origin of PDGF-B determines its profibrotic effect in the kidney. Increased PDGF-B expression in injured maladaptive tubular epithelial cells was identified as the major origin and driver of kidney fibrosis via paracrine signaling to peritubular fibroblasts, initiating the creation of interstitial fibrotic niches (i.e., spatially confined areas of fibrogenesis). Our study also identified a molecular paracrine mechanism of tubular injury–initiated interstitial fibrosis.

We found, in both mice and humans, that tubular PDGF-B and interstitial PDGFR-β are spatially associated. Although it is unclear whether PDGF-B induces its receptor in the

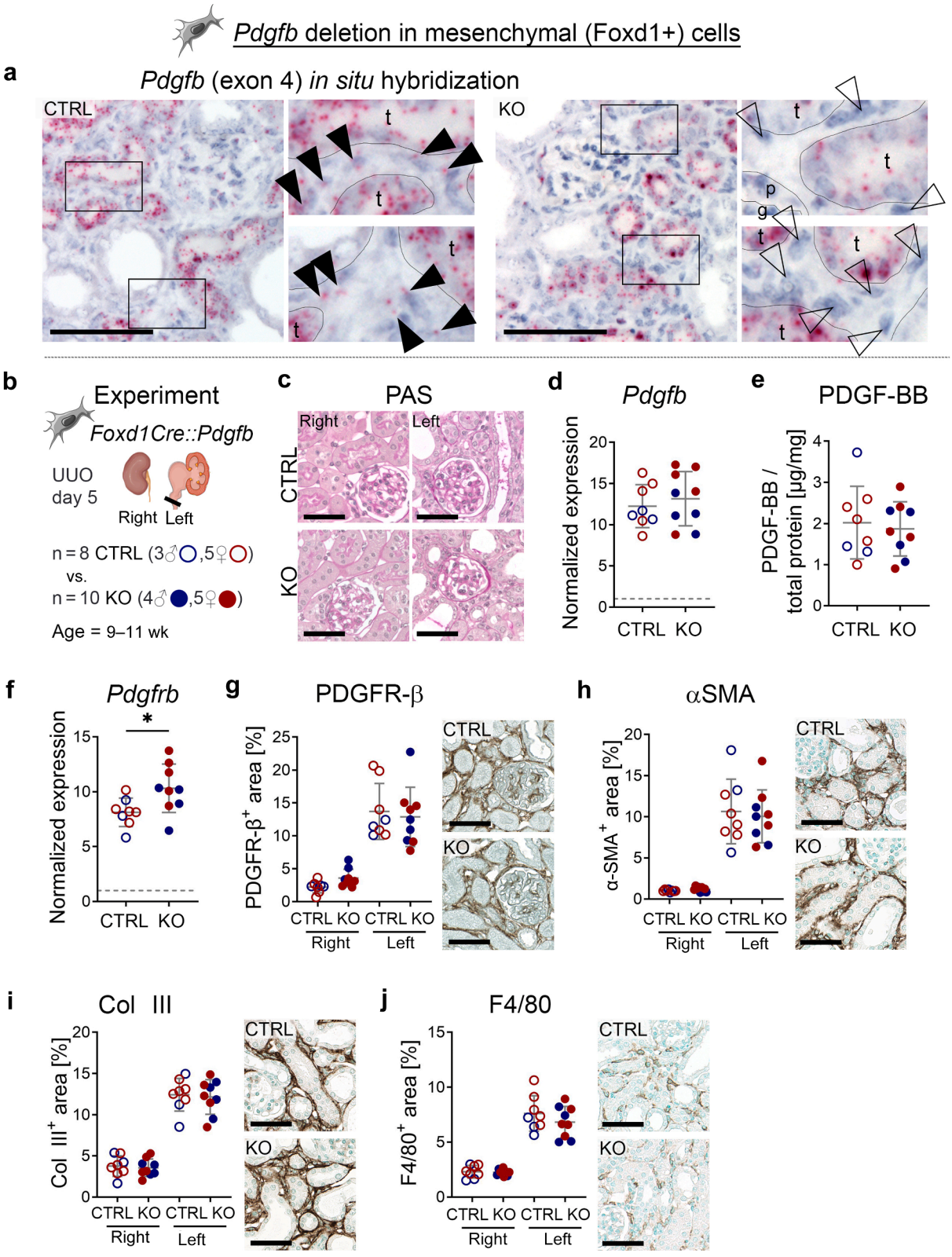


Figure 7 | Unilateral ureteral obstruction (UUO) in *Foxd1Cre::Pdgfb* mice. (**a**) Red *in situ* hybridization stainings depict *Pdgfb* expression in histologic samples from UUO mice of the *Foxd1Cre::Pdgfb* line. For better visualization, structures are outlined in the close-up images. Black arrow indicates positive interstitial cell, and blank arrow indicates negative interstitial cell. (**b**) Experimental design. At the age of 9 to 11 weeks, 8 wild-type–like control (CTRL) animals are compared with 9 mice with *Pdgfb* deletion specifically in mesenchymal Forkhead box d1 (Foxd1)–positive cells (knockout [KO]). Males are shown in blue, and females are shown in red. (**c**) Periodic acid–Schiff (PAS)–stained kidney histology does not show any abnormalities in the KO mice. (**d**) *Pdgfb* mRNA expression is similar between the groups, whereas (continued)

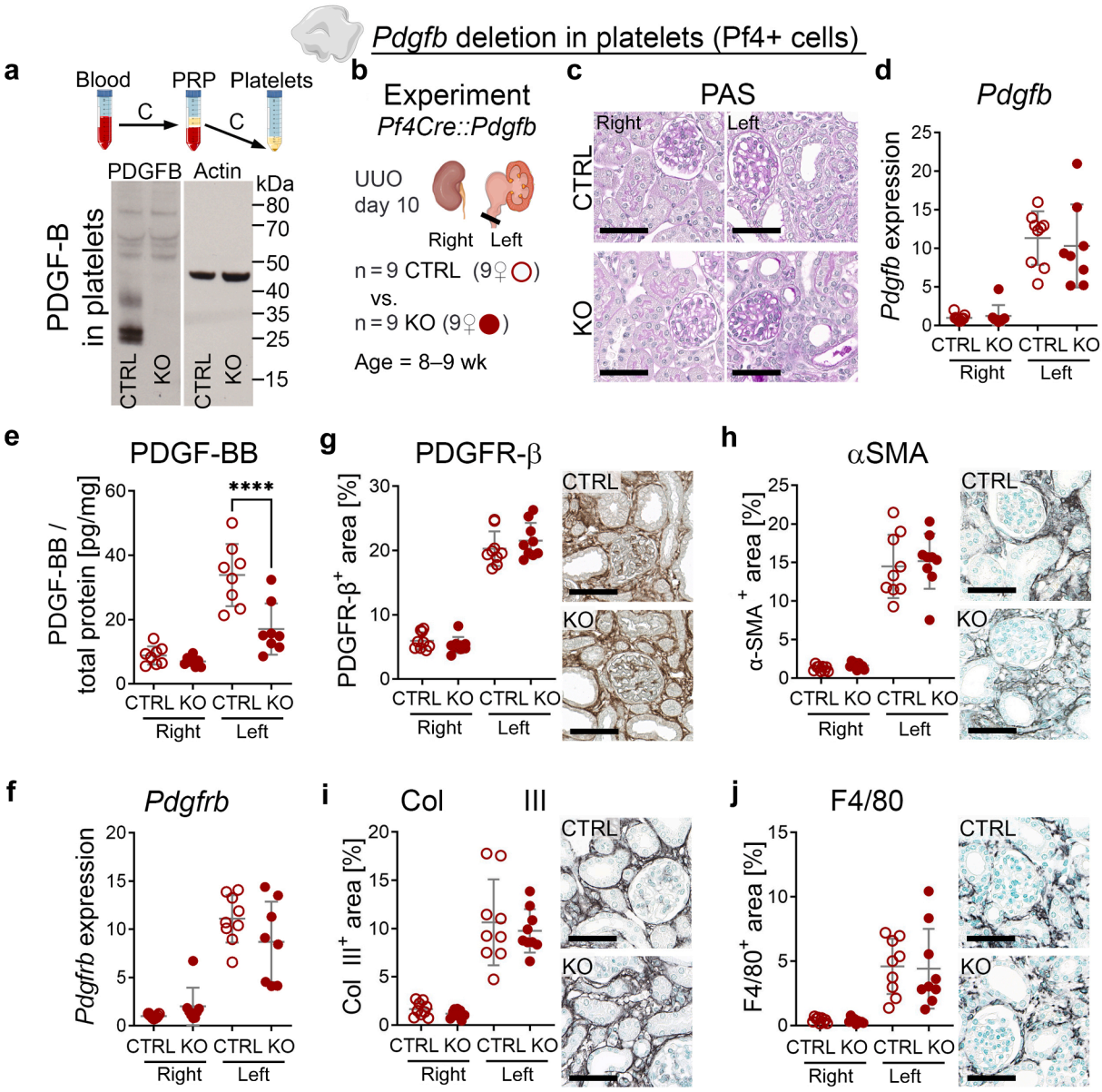


Figure 8 | Unilateral ureteral obstruction (UUO) in *Pf4Cre::Pdgfb* mice. (**a**) Western blot of isolated platelets confirms the deletion of platelet-derived growth factor-B (PDGF-B) in platelets. (**b**) Experimental design of the UUO experiment. At the age of 8 to 9 weeks, 9 control (CTRL) animals are compared with 9 knockout (KO) mice. (**c**) Periodic acid–Schiff (PAS)–stained kidney histology does not show any differences between the groups. (**d**) Cortex *Pdgfb* mRNA expression is similar between the groups, whereas (**e**) KO mice have significantly reduced amounts of PDGF-BB protein in the UUO kidneys. However, (**f**) *Pdgfrb* is similar and immunostainings reveal similar a expression of (**g**) PDGF receptor (PDGFR)–β, (**h**) α-smooth muscle actin (α-SMA), (**i**) collagen (Col) type III, and (**j**) F4/80. ****$P < 0.0001$ (analysis of variance or Kruskal-Wallis). Bar = 50 μm. C, centrifugation; Pf4, platelet factor 4; PRP, platelet-rich plasma. To optimize viewing of this image, please see the online version of this article at www.kidney-international.org.

interstitial cells or whether PDGFR-ß–positive cells migrate along a gradient, bioinformatic analyses confirmed an increased interaction between *PDGFB*$^{+}$ proximal tubules and fibroblasts, whereas this was not the case for *PDGFB*$^{-}$ tubules or healthy samples. These fibrotic niches of interstitial cells were already observed in association with a single PDGF-B–expressing tubular cell. Our analysis of ligand-receptor interactions identified several ECM-integrin connections

Figure 7 | (continued) (**e**) *Pdgfrb* was higher in the KO mice. Immunostainings, however, reveal similar expression of (**f**) platelet-derived growth factor receptor (PDGFR)–β, (**g**) α-smooth muscle actin (α-SMA), (**h**) collagen (Col) type III, and (**i**) F4/80. *$P < 0.05$ (analysis of variance or Kruskal-Wallis). Bar = 50 μm. G, glomerular tuft; p, parietal epithelial cell; PDGF, platelet-derived growth factor; t, positive tubule. To optimize viewing of this image, please see the online version of this article at www.kidney-international.org.

between *PDGFB*$^+$ tubules and *PDGFRB*$^+$ fibroblasts, supporting the formation of a profibrotic niche via direct interaction of these cells. Past studies have shown that PDGF-BB stimulation upregulates integrin expression in fibroblasts of different origin *in vitro*.[36–38] *Vice versa*, integrins can directly interact with PDGFR-β, thereby controlling and potentiating the downstream signal cascade and enhancing cell proliferation, migration, and survival.[1,39] For example, in breast cancer, integrin α11 promotes cancer-associated fibroblast invasion and cancer-associated fibroblast–induced tumor cell invasion via interaction with PDGFR-β in a ligand-dependent manner and promotion of downstream c-Jun N-terminal kinase activation, leading to the production of tenascin C.[40] We also found tenascin C to be expressed in the niches and to be among the major ligand-receptor interactions between tubules and fibroblasts. This is in line with previous findings identifying tenascin C as a major constituent of the fibrogenic niches promoting fibroblast proliferation in kidneys[41] and facilitator of acute kidney injury–to–chronic kidney disease transition.[42] Previously, *in vitro* studies showed significant induction of tenascin C expression after PDGF-B stimulation of intestinal myofibroblasts.[43] Like other ECM proteins, such as fibronectin and collagen, tenascin C itself has a growth factor–binding domain that binds PDGF, locally enhancing the availability of the ligand.[44,45] Although we have no experimental evidence of how much PDGF in the kidney is matrix bound, even a small proportion of bound ligand in the spatially confined niche would have the ability to establish localized signaling hubs. This could amplify cosignaling between integrins and PDGFR-β, which is crucial in regulating fibroblast activation.[46] Such mechanisms are consistent with the observed TNC- and integrin-enriched interaction patterns. Overall, our results indicate that the PDGF-B–PDGFR-β signaling axis between proximal tubules and interstitial mesenchymal cells leads to the early activation of (myo)fibroblasts in kidney fibrosis.

Transcription factor activity analysis in PDGFB$^+$ versus PDGFB$^-$ PTs identified several factors that were predicted to regulate *PDGFB* and could be responsible for its tubular expression. For example, FOXO1 was described to be induced in tubular cells by oxidative stress or high glucose.[47] In venous endothelial cells, FOXO1, as a downstream molecular signaling pathway of protein kinase B, directly regulated *PDGFB* expression.[48] Similarly, CEBPB can also be induced by metabolic stress and ischemia and was shown to facilitate *PDGFB* transcription by direct interaction with *PDGFB* promoter elements in gastric cancer cells.[49] TEAD1, together with Yes-associated protein 1, triggered *PDGFB* transcription in bladder cancer cells.[50] In tubular epithelial cells, TEAD1 was upregulated during experimental cisplatin-induced acute kidney injury.[51] Overall, these studies suggest that cell stress, induced by different stimuli, upregulates *PDGFB* via these transcriptional regulators in tubular epithelial cells.

Doublecortin domain-containing 2 was among the most significantly upregulated genes in *PDGFB*$^+$ tubules. Although not much is known about the functional role of this protein, it was previously identified as a marker in maladaptive (failed repair) tubular cells, similar to, but more specific than, vascular cell adhesion protein 1 (VCAM-1).[25,34] In line with this, PDGFB$^+$ PTs exhibited downregulation of physiological, mostly metabolic, pathways. Consistently, we observed a significantly reduced expression of doublecortin domain-containing 2 and other markers of injured PTs (i.e., Kim-1) in the *Pax8Cre::Pdgfb* KO mice after UUO. Although Kim-1 was always reduced in the KO mice, we detected similar expression of the tubular injury marker neutrophil gelatinase–associated lipocalin in all 3 models in the *Pax8-Cre::Pdgfb* line. This could suggest segment-specific effects, because neutrophil gelatinase–associated lipocalin is mostly expressed by distal tubules, whereas Kim-1 expression is highest in proximal tubules. However, the reduction of the interstitium in old animals occurred primarily in the medulla but not in the cortex. It is more likely that the models damage different nephron segments to varying degrees, resulting in differences in the injury markers.[52,53]

Inflammation is always closely linked to disease progression and fibrosis formation, and numerous studies have shown that the progression of fibrosis can be reduced by anti-inflammatory treatments. Surprisingly, we could not detect any differences in inflammatory markers in the *Pax8Cre::Pdgfb* line, underscoring the role of direct tubule-fibroblast crosstalk. A recent multiomic study identified an inflammatory and profibrotic tubular cell phenotype (*HAVCR1*$^+$*VCAM1*$^+$*ICAM1*$^+$) in human and murine samples, which expressed *PDGFB* and was associated with leukocyte recruitment and myofibroblast activation.[54] Our results indicate that deletion of *Pdgfb* in tubules is sufficient to modulate the fibrogenic niche and reduce fibrosis without significant effects on inflammation.

Here, we found that despite expression of PDGF-B in different cell populations, only tubular cell–derived PDGF-B drove fibrotic disease. The coexpression of PDGFR-β and PDGF-B in renal mesenchymal cells, particularly pericytes, suggested a potential autocrine stimulation of interstitial cells, which also occurs in some malignancies (e.g., certain gliomas, sarcomas, or leukemias).[55–57] In tumor biology, PDGF can have a dual mode of action: an autocrine loop required for cell migration, invasion, and metastatic dissemination and paracrine signaling to support the tumor microenvironment (i.e., blood vessel functionality and recruitment of cancer-associated fibroblasts).[1,58,59] However, our data argue against a role of autocrine PDGF-B signaling in kidney fibrosis. The expression analysis in our models suggested that 1 explanation might be the low amount of mesenchymal-derived PDGF-B compared with the tubular source.

The situation is different when it comes to platelets, which are an important source of PDGF-B. It is stored in high

concentrations in α-granules, which are released on platelet activation[27] and were shown to mediate (e.g., wound healing).[60] There is an ongoing debate about the role of platelets in the development and progression of kidney diseases and the role of the released PDGF and other proinflammatory and profibrotic factors in amplifying kidney injury.[61] Also, in the liver, PDGF-B secreted by platelets promoted liver fibrosis.[62] Although a recent publication showed, by using *Pf4Cre::Pdgfb* mice, that the PDGF-B reservoir in platelets maintains vascular integrity by recruitment of pericytes in the tumor microvasculature,[63] we did not observe any differences in PDGFR-β or α-SMA levels in either healthy or fibrotic kidneys. Our data showed that platelet-derived PDGF-B is dispensable for kidney fibrosis in the UUO model, potentially suggesting at best a minor role of platelets in tubulointerstitial fibrosis. However, this might be specific to the model, and we cannot exclude that platelet-derived PDGF-B plays a role in fibrosis development in models (or diseases) with considerable (or primary) microvascular injury, such as thrombotic microangiopathies.

The first International Society of Nephrology consensus guidelines for preclinical animal studies proposed study designs making results more translationally robust.[64] Our study tackled several of these, analyzing both young and old mice in each transgenic line, showing that the effects were sex independent, consistently using wild-type littermates as controls, and robustly confirming the effects in 3 pathophysiologically distinct models of kidney fibrosis.

Our study has limitations. We have not analyzed other PDGF-B sources, such as from immune or endothelial cells. Given that mice with a constitutive deletion of *Pdgfb* in endothelial cells are not viable, this prevented us from performing such experiments. Although the sequencing data from the *Pax8Cre::Pdgfb* mice showed a downregulation of mitogen-activated protein kinase and phosphatidylinositol-3′-kinase pathways, other profibrotic pathways (i.e., transforming growth factor-β and epidermal growth factor receptor) were simultaneously activated in the KO. Because the bulk RNA data do not provide information on which cells influence the signaling pathway, we cannot discern the exact cellular sources of the pathophysiological processes. However, although KO mice might show a compensatory upregulation of transforming growth factor-β as an upstream regulator of PDGF,[65,66] fibrosis was still reduced. Although the Pax8-Cre mouse line has been widely used by us and others before,[67,68] we could neither control whether recombination was equally efficient across all nephron segments nor exclude that the expression of the Cre recombinase in the KO mice (i.e., high levels of a nonphysiological protein) has some toxic adverse effects, as was shown for other Cre drivers.[69,70]

In conclusion, our data show that kidney epithelial cells are the major source of PDGF-B in fibrosis mediating paracrine profibrotic signaling to the peritubular mesenchyme. This cellular crosstalk mediates the initiation of interstitial profibrotic niches and drives kidney fibrosis.

DISCLOSURE

All the authors declared no competing interests.

DATA STATEMENT

The data generated or analyzed in this study were included in the main document and supplementary information files of this article. Transcriptomic data for reanalysis were derived from https://www.ncbi.nlm.nih.gov/geo/query/acc.cgi?acc=GSE182256 (murine unilateral ureteral obstruction) and https://www.kpmp.org/ (human). Own transcriptomic data from the transgenic mouse line can be accessed via GSE312904 and GSE312905. For gene set enrichment analysis, https://rdrr.io/bioc/clusterProfiler/man/GSEA.html was used. Other original data are available on request from the authors.

ACKNOWLEDGMENTS

We are especially thankful for great technical support from Jana Baues, Simon Otten, Marie Cherelle Timm, Christina Gianussis, Louisa Böttcher, and Pinar Sönmez.

This work was supported by the IZKF Genomics facility, a core facility of the Interdisciplinary Center for Clinical Research Aachen within the Faculty of Medicine at RWTH Aachen University.

FUNDING STATEMENT

This study was funded by the German Research Foundation (DFG; Project-IDs 322900939, 454024652, and 432698239 to PB and 445703531 to BMK, RK, JF, and PB), the European Research Council (ERC; Consolidator Grant AIM.imaging.CKD, number 101001791 to PB), and the Federal Ministry of Education and Research (STOP-FSGS-01GM2202C; to PB).

AUTHOR CONTRIBUTIONS

BMK and PB designed the study and interpreted the data. BMK and EMB performed animal experiments. TC performed stainings. SM, DWLW, and MG performed bulk and single-cell RNA-sequencing analysis. DLH and RDB performed pathomics analysis. BMK drafted the manuscript and figures. RK, SH, JF, and PB provided conceptual support, advised on data interpretation, and edited the manuscript. All authors edited and approved the final version of the manuscript.

Supplementary material is available online at www.kidney-international.org.

REFERENCES

1. Andrae J, Gallini R, Betsholtz C. Role of platelet-derived growth factors in physiology and medicine. *Genes Dev*. 2008;22:1276–1312.
2. Floege J, Eitner F, Alpers CE. A new look at platelet-derived growth factor in renal disease. *J Am Soc Nephrol*. 2008;19:12–23.
3. Klinkhammer BM, Floege J, Boor P. PDGF in organ fibrosis. *Mol Aspects Med*. 2018;62:44–62.
4. Lindahl P, Hellstrom M, Kalen M, et al. Paracrine PDGF-B/PDGF-Rbeta signaling controls mesangial cell development in kidney glomeruli. *Development*. 1998;125:3313–3322.
5. Betsholtz C. Insight into the physiological functions of PDGF through genetic studies in mice. *Cytokine Growth Factor Rev*. 2004;15:215–228.
6. Enge M, Bjarnegard M, Gerhardt H, et al. Endothelium-specific platelet-derived growth factor-B ablation mimics diabetic retinopathy. *EMBO J*. 2002;21:4307–4316.
7. Bjarnegard M, Enge M, Norlin J, et al. Endothelium-specific ablation of PDGFB leads to pericyte loss and glomerular, cardiac and placental abnormalities. *Development*. 2004;131:1847–1857.
8. Leveen P, Pekny M, Gebre-Medhin S, et al. Mice deficient for PDGF B show renal, cardiovascular, and hematological abnormalities. *Genes Dev*. 1994;8:1875–1887.
9. Wu H, Uchimura K, Donnelly EL, et al. Comparative analysis and refinement of human PSC-derived kidney organoid differentiation with single-cell transcriptomics. *Cell Stem Cell*. 2018;23:869–881.e8.

10. Ostendorf T, Boor P, van Roeyen CR, et al. Platelet-derived growth factors (PDGFs) in glomerular and tubulointerstitial fibrosis. *Kidney Int Suppl (2011)*. 2014;4:65–69.
11. Chen YT, Chang FC, Wu CF, et al. Platelet-derived growth factor receptor signaling activates pericyte-myofibroblast transition in obstructive and post-ischemic kidney fibrosis. *Kidney Int*. 2011;80:1170–1181.
12. Boor P, Konieczny A, Villa L, et al. PDGF-D inhibition by CR002 ameliorates tubulointerstitial fibrosis following experimental glomerulonephritis. *Nephrol Dial Transplant*. 2007;22:1323–1331.
13. Floege J, Eng E, Young BA, et al. Infusion of platelet-derived growth factor or basic fibroblast growth factor induces selective glomerular mesangial cell proliferation and matrix accumulation in rats. *J Clin Invest*. 1993;92:2952–2962.
14. Floege J, Ostendorf T, Janssen U, et al. Novel approach to specific growth factor inhibition *in vivo*: antagonism of platelet-derived growth factor in glomerulonephritis by aptamers. *Am J Pathol*. 1999;154:169–179.
15. Jia T, Xu T, Smeets B, et al. The role of platelet-derived growth factor in focal segmental glomerulosclerosis. *J Am Soc Nephrol*. 2023;34:241–257.
16. Bouchard M, Souabni A, Busslinger M. Tissue-specific expression of cre recombinase from the Pax8 locus. *Genesis*. 2004;38:105–109.
17. Humphreys BD, Lin SL, Kobayashi A, et al. Fate tracing reveals the pericyte and not epithelial origin of myofibroblasts in kidney fibrosis. *Am J Pathol*. 2010;176:85–97.
18. Tiedt R, Schomber T, Hao-Shen H, et al. Pf4-Cre transgenic mice allow the generation of lineage-restricted gene knockouts for studying megakaryocyte and platelet function *in vivo*. *Blood*. 2007;109:1503–1506.
19. Ehling J, Babickova J, Gremse F, et al. Quantitative micro-computed tomography imaging of vascular dysfunction in progressive kidney diseases. *J Am Soc Nephrol*. 2016;27:520–532.
20. Djudjaj S, Papasotiriou M, Bulow RD, et al. Keratins are novel markers of renal epithelial cell injury. *Kidney Int*. 2016;89:792–808.
21. Bouteldja N, Klinkhammer BM, Bulow RD, et al. Deep learning-based segmentation and quantification in experimental kidney histopathology. *J Am Soc Nephrol*. 2021;32:52–68.
22. Holscher DL, Bouteldja N, Joodaki M, et al. Next-generation morphometry for pathomics-data mining in histopathology. *Nat Commun*. 2023;14:470.
23. Holscher DL, Goedertier M, Klinkhammer BM, et al. tRigon: an R package and Shiny App for integrative (path-)omics data analysis. *BMC Bioinformatics*. 2024;25:98.
24. Doke T, Abedini A, Aldridge DL, et al. Single-cell analysis identifies the interaction of altered renal tubules with basophils orchestrating kidney fibrosis. *Nat Immunol*. 2022;23:947–959.
25. Lake BB, Menon R, Winfree S, et al. An atlas of healthy and injured cell states and niches in the human kidney. *Nature*. 2023;619:585–594.
26. Betsholtz C, Lindblom P, Bjarnegard M, et al. Role of platelet-derived growth factor in mesangium development and vasculopathies: lessons from platelet-derived growth factor and platelet-derived growth factor receptor mutations in mice. *Curr Opin Nephrol Hypertens*. 2004;13:45–52.
27. Ross R, Glomset J, Kariya B, et al. A platelet-dependent serum factor that stimulates the proliferation of arterial smooth muscle cells *in vitro*. *Proc Natl Acad Sci U S A*. 1974;71:1207–1210.
28. Lindblom P, Gerhardt H, Liebner S, et al. Endothelial PDGF-B retention is required for proper investment of pericytes in the microvessel wall. *Genes Dev*. 2003;17:1835–1840.
29. Schubert M, Klinger B, Klunemann M, et al. Perturbation-response genes reveal signaling footprints in cancer gene expression. *Nat Commun*. 2018;9:20.
30. Polonsky M, Gerhardt LMS, Yun J, et al. Spatial transcriptomics defines injury specific microenvironments and cellular interactions in kidney regeneration and disease. *Nat Commun*. 2024;15:7010.
31. Cheneby J, Gheorghe M, Artufel M, et al. ReMap 2018: an updated atlas of regulatory regions from an integrative analysis of DNA-binding ChIP-seq experiments. *Nucleic Acids Res*. 2018;46:D267–D275.
32. Kolmykov S, Yevshin I, Kulyashov M, et al. GTRD: an integrated view of transcription regulation. *Nucleic Acids Res*. 2021;49:D104–D111.
33. Liska O, Bohar B, Hidas A, et al. TFLink: an integrated gateway to access transcription factor-target gene interactions for multiple species. *Database (Oxford)*. 2022;2022:baac083.
34. Janosevic D, De Luca T, Kidney Precision Medicine Project, Eadon MT. The Kidney Precision Medicine Project and single-cell biology of the injured proximal tubule. *Am J Pathol*. 2025;195:7–22.
35. Abedini A, Levinsohn J, Klotzer KA, et al. Single-cell multi-omic and spatial profiling of human kidneys implicates the fibrotic microenvironment in kidney disease progression. *Nat Genet*. 2024;56:1712–1724.
36. Xu J, Clark RA. Extracellular matrix alters PDGF regulation of fibroblast integrins. *J Cell Biol*. 1996;132:239–249.
37. Ahlen K, Rubin K. Platelet-derived growth factor-BB stimulates synthesis of the integrin alpha 2-subunit in human diploid fibroblasts. *Exp Cell Res*. 1994;215:347–353.
38. Nesbit M, Schaider H, Berking C, et al. Alpha5 and alpha2 integrin gene transfers mimic the PDGF-B-induced transformed phenotype of fibroblasts in human skin. *Lab Invest*. 2001;81:1263–1274.
39. Schneller M, Vuori K, Ruoslahti E. Alphavbeta3 integrin associates with activated insulin and PDGFbeta receptors and potentiates the biological activity of PDGF. *EMBO J*. 1997;16:5600–5607.
40. Primac I, Maquoi E, Blacher S, et al. Stromal integrin alpha11 regulates PDGFR-beta signaling and promotes breast cancer progression. *J Clin Invest*. 2019;129:4609–4628.
41. Fu H, Tian Y, Zhou L, et al. Tenascin-C is a major component of the fibrogenic niche in kidney fibrosis. *J Am Soc Nephrol*. 2017;28:785–801.
42. Zhu H, Liao J, Zhou X, et al. Tenascin-C promotes acute kidney injury to chronic kidney disease progression by impairing tubular integrity via alphavbeta6 integrin signaling. *Kidney Int*. 2020;97:1017–1031.
43. Islam MS, Kusakabe M, Horiguchi K, et al. PDGF and TGF-beta promote tenascin-C expression in subepithelial myofibroblasts and contribute to intestinal mucosal protection in mice. *Br J Pharmacol*. 2014;171:375–388.
44. De Laporte L, Rice JJ, Tortelli F, et al. Tenascin C promiscuously binds growth factors via its fifth fibronectin type III-like domain. *PLoS One*. 2013;8:e62076.
45. Somasundaram R, Schuppan D. Type I, II, III, IV, V, and VI collagens serve as extracellular ligands for the isoforms of platelet-derived growth factor (AA, BB, and AB). *J Biol Chem*. 1996;271:26884–26891.
46. Ivaska J, Heino J. Cooperation between integrins and growth factor receptors in signaling and endocytosis. *Annu Rev Cell Dev Biol*. 2011;27:291–320.
47. Zhang M, Dong W, Li Z, et al. Effect of forkhead box O1 in renal tubular epithelial cells on endotoxin-induced acute kidney injury. *Am J Physiol Renal Physiol*. 2021;320:F262–F272.
48. Uebelhoer M, Natynki M, Kangas J, et al. Venous malformation-causative TIE2 mutations mediate an AKT-dependent decrease in PDGFB. *Hum Mol Genet*. 2013;22:3438–3448.
49. Du S, Yang Z, Lu X, et al. Anoikis resistant gastric cancer cells promote angiogenesis and peritoneal metastasis through C/EBPbeta-mediated PDGFB autocrine and paracrine signaling. *Oncogene*. 2021;40:5764–5779.
50. Wang KJ, Wang C, Dai LH, et al. Targeting an autocrine regulatory loop in cancer stem-like cells impairs the progression and chemotherapy resistance of bladder cancer. *Clin Cancer Res*. 2019;25:1070–1086.
51. Tran M, Jiao B, Du H, et al. TEAD1 prevents necroptosis and inflammation in cisplatin-induced acute kidney injury through maintaining mitochondrial function. *Int J Biol Sci*. 2025;21:565–578.
52. Lieberthal W, Nigam SK. Acute renal failure, I: relative importance of proximal vs. distal tubular injury. *Am J Physiol*. 1998;275:F623–F631.
53. Forbes MS, Thornhill BA, Minor JJ, et al. Fight-or-flight: murine unilateral ureteral obstruction causes extensive proximal tubular degeneration, collecting duct dilatation, and minimal fibrosis. *Am J Physiol Renal Physiol*. 2012;303:F120–F129.
54. Reck M, Baird DP, Veizades S, et al. Multiomic analysis of human kidney disease identifies a tractable inflammatory and pro-fibrotic tubular cell phenotype. *Nat Commun*. 2025;16:4745.
55. Lokker NA, Sullivan CM, Hollenbach SJ, et al. Platelet-derived growth factor (PDGF) autocrine signaling regulates survival and mitogenic pathways in glioblastoma cells: evidence that the novel PDGF-C and PDGF-D ligands may play a role in the development of brain tumors. *Cancer Res*. 2002;62:3729–3735.
56. Dai C, Celestino JC, Okada Y, et al. PDGF autocrine stimulation dedifferentiates cultured astrocytes and induces oligodendrogliomas and oligoastrocytomas from neural progenitors and astrocytes *in vivo*. *Genes Dev*. 2001;15:1913–1925.

57. Yang J, Liu X, Nyland SB, et al. Platelet-derived growth factor mediates survival of leukemic large granular lymphocytes via an autocrine regulatory pathway. *Blood*. 2010;115:51–60.
58. Kuzmanov A, Hopfer U, Marti P, et al. LIM-homeobox gene 2 promotes tumor growth and metastasis by inducing autocrine and paracrine PDGF-B signaling. *Mol Oncol*. 2014;8:401–416.
59. Ostman A. PDGF receptors-mediators of autocrine tumor growth and regulators of tumor vasculature and stroma. *Cytokine Growth Factor Rev*. 2004;15:275–286.
60. Pierce GF, Mustoe TA, Lingelbach J, et al. Platelet-derived growth factor and transforming growth factor-beta enhance tissue repair activities by unique mechanisms. *J Cell Biol*. 1989;109:429–440.
61. Zoja C, Remuzzi G. Role of platelets in progressive glomerular diseases. *Pediatr Nephrol*. 1995;9:495–502.
62. Yoshida S, Ikenaga N, Liu SB, et al. Extrahepatic platelet-derived growth factor-beta, delivered by platelets, promotes activation of hepatic stellate cells and biliary fibrosis in mice. *Gastroenterology*. 2014;147:1378–1392.
63. Zhang Y, Cedervall J, Hamidi A, et al. Platelet-specific PDGFB ablation impairs tumor vessel integrity and promotes metastasis. *Cancer Res*. 2020;80:3345–3358.
64. Nangaku M, Kitching AR, Boor P, et al. International Society of Nephrology first consensus guidance for preclinical animal studies in translational nephrology. *Kidney Int*. 2023;104:36–45.
65. Taylor LM, Khachigian LM. Induction of platelet-derived growth factor B-chain expression by transforming growth factor-beta involves transactivation by Smads. *J Biol Chem*. 2000;275:16709–16716.
66. Porsch H, Mehic M, Olofsson B, et al. Platelet-derived growth factor beta-receptor, transforming growth factor beta type I receptor, and CD44 protein modulate each other's signaling and stability. *J Biol Chem*. 2014;289:19747–19757.
67. Djudjaj S, Martin IV, Buhl EM, et al. Macrophage migration inhibitory factor limits renal inflammation and fibrosis by counteracting tubular cell cycle arrest. *J Am Soc Nephrol*. 2017;28:3590–3604.
68. Kuppe C, van Roeyen C, Leuchtle K, et al. Investigations of glucocorticoid action in GN. *J Am Soc Nephrol*. 2017;28:1408–1420.
69. Rashbrook VS, Brash JT, Ruhrberg C. Cre toxicity in mouse models of cardiovascular physiology and disease. *Nat Cardiovasc Res*. 2022;1:806–816.
70. Frahsek M, Schulte K, Chia-Gil A, et al. Cre recombinase toxicity in podocytes: a novel genetic model for FSGS in adolescent mice. *Am J Physiol Renal Physiol*. 2019;317:F1375–F1382.